3D printing of vacuum and pressure tight polymer vessels for thermally driven chillers and heat pumps

3D printing of vacuum and pressure tight polymer vessels for thermally driven chillers and heat pumps

Shihab AL-Hasni [a], Giulio Santori [a]

[a] The University of Edinburgh, School of Engineering, Institute for Materials and Processes, Sanderson Building, The King's Buildings, Mayfield Road, EH9 3BF Edinburgh, Scotland, UK

Abstract

Adsorption chillers and heat pumps are thermally driven devices working under vacuum or pressure depending on the working fluids. Their production involves a combination of special manufacturing processes that affect their final cost and eventually their technology readiness level. Conversely, 3D printing is a simple manufacturing process where parts are created directly from a 3D computer model. Therefore, enabling 3D printing for adsorption chillers and heat pumps manufacturing can facilitate technology commercialization. Unfortunately, 3D printed objects are often porous and show limited pressure and vacuum tightness. In this study we compare two different 3D printing processes (Stereolitography and Fused Deposition Modelling) to manufacture vacuum and pressure tight vessels. These two straightforward and easy-to-replicate manufacturing processes enable the realization of vacuum and pressure tight, porosity-free vessels. Tightness is demonstrated at pressures up to ~400 kPa and vacuum down to 1 kPa.

1. Introduction

Adsorption chillers and heat pumps (adsorption heat transformers) have huge potential for emissions reduction but are in practice not ready for the market [1,2]. The units currently marketed are similar more to R&D prototypes than commercial devices and are available at prices which cannot compete with vapour compression systems [3]. Two shortcomings, among other factors, are unsolved:
1) the operating pressures: adsorption heat transformers (AHTs) work in vacuum or high pressure depending on the refrigerant fluid [4] (water: 0.8-7 kPa, ethanol: 2-18 kPa, ammonia: 500-1500kPa). Vacuum AHTs show unavoidable loss of tightness and the need of restoring vacuum and refrigerant fluid periodically. High pressure AHTs work with ammonia, remain tight longer but still need of periodical refilling and all the parts need to be in steel since ammonia is not compatible with highly thermal conductive copper or copper alloys;

2) Manufacturing: AHTs are never lightweight and require laborious manufacture. Vacuum AHTs follow strict vacuum standards and rely on machined and special-welded components of steel or aluminium [5]. Pressure AHTs use steel, resulting in heavy components.

3D printing is a recent manufacturing technique [6,7] that holds the promise for a revolution in the manufacturing sector. Unfortunately, 3D printed objects are deemed unsuitable for the containment of fluids due to their high porosity. The two most popular 3D printing techniques are fused deposition modelling (FDM) and stereolithography (SLA) [8]. FDM is a continuous process consisting of melting a variable amount of thermoplastic polymer that is extruded through a nozzle on a build plate. SLA uses a focused laser beam on a layer of epoxy-based resin that is then polymerized. SLA requires post-curing under UV light to complete the polymerization reaction and finish the 3D printed object [8]. 3D printing has helped manufacturers to create prototypes rapidly and low cost compared to a number of other established processes [6,7,9,10]. 3D printing starts from a 3D computer model, therefore objects of any shape can be virtually produced [11,12]. Each 3D printer has its own slicing software that provides an insight into the 3D printing settings and also includes a simulation of the 3D printing process [12]. Although 3D printing is a promising manufacturing process, the manufactured parts are often not vacuum or pressure tight [13–15]. The tuning of the slicing process is key to minimize the porosity. As such, Table 1 shows some of the 3D printing settings that can affect the porosity level while printing an object.

Table 1 some of the 3D printing parameters that can reduce the porosity of 3D printed objects.

Parameter	Description	Type	Source
Layer height	The layer elevation in each 3D printing step, the elevation between the fused deposited layers.	SLA, FDM	[16,17]
Extrusion flow	The amount of flowing filament per unit time during the 3D printing process.	FDM	[6,13]
Printing speed	An increase of printing speed could decreases the quality of the overall print. This variable is usually altered to gain highly defined objects.	FDM	[13]
Printing temperature	This parameter is used to increase or decrease the interlayer adhesion of 3D printing filament.	FDM	[6,18]
Live z-axis level	This function is essential as the wrong z-axis level will result in a weak structure of a 3D printed part.	SLA, FDM	[19,20]
Shell	This parameter is tuned to strengthen the 3D printed part in terms of rigidity.	FDM	[21]
Seam	The end point of each 3D printed layer, it can be randomised or fixed.	FDM	[13]

The porosity of the manufactured object is directly correlated to its leaks. Therefore, after manufacturing, the tightness has to be quantified to check that it is within the level allowed in each

specific application. Various leak detection methods exist [22–24] and among them pressure rise/drop [25–27] is a straightforward method applicable to check the tightness of 3D printed vessels.

The pioneering investigation [13] suggested that the amount molten plastic flow (extrusion flow) is crucial to produce air-tight 3D printed parts. In [13] ABS and Nylon were tested through immersion of 3D printed tubes in a bubble bath. The main recommendation from this investigation consisted of printing cylindrical shape vessels, start with 2.0 mm wall thickness and gradually increase the extrusion flow as explained in Fig. 1.

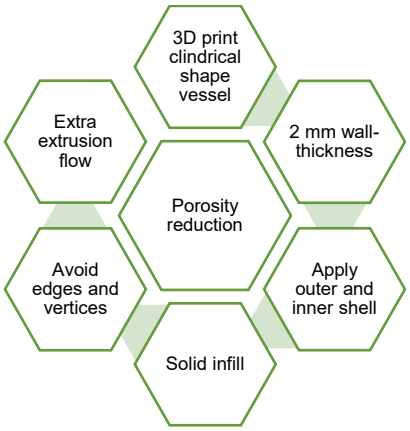

Figure 1: Summary of variables that could assist in the reduction of the porosity of a 3D printed part by FDM [13].

However, all the tests in [13] used the bubble method which does not provide an adequate indication of tightness. Bubble test technique can detect only large leaks and fail to detect smaller leaks that are those to be checked for AHT. Furthermore, the investigation in [13] was qualitative and did not refer to any existing quantitative leak rate classification. The definition of leak rate q is [26]:

$$q = \frac{\Delta P \, \mathrm{V}}{\Delta t} \tag{1}$$

Where ΔP is the difference between the pressure [Pa] at time t_0 [s] and time $t_1=t+\Delta t$, V [m^3] is the internal volume of a confined space that has to be tested and Δt is the measurement interval [s]. According to the tightness classification in [26] and reported for convenience in Table 2, bubble tests are adequate for the detection of leaks at rates >10^{-5} Pa m^3 s^{-1}. AHTs would require instead vessels that are leak tested at rates <10^{-7} Pa m^3 s^{-1}.

Table 2 Classification of systems tightness based on leak rate.

	Leaky	Tight	Very tight
Leak rate of a system [Pa m^3 s^{-1}]	> 10^{-5}	< 10^{-6} and > 10^{-7}	< 10^{-7}

Furthermore, real devices need to be very tight at pressures well above the 150kPa tested in [13] and under vacuum in between 1 kPa and 10 kPa. These conditions have not been demonstrated yet. In this investigation we develop a method to produce pressure and vacuum tight vessels using 3D printing technology which is suitable for AHTs.

2. Materials and methods

3D printing: the enclosed Desktop FDM 3D printer Zortrax M200 (Zortrax, Poland) with 0.4 mm diameter nozzle and the SLA 3D printer Formlabs 1 (Formlabs GmbH, Germany) were used to manufacture the vessels. These facilities are available at the U-create studio of The University of Edinburgh (United Kingdom). For both the 3D printers, 3D models of the vessels were created in Fusion 360 (Autodesk, United Kingdom).

As far as FDM 3D printing is concerned, the 3D models were processed by using the slicer software Z-suite (Zortrax, Poland). The slicer was used to virtually adjust the 3D model over the build plate and to prevent printing outside the printing area. Automatic 3D printing support up to 45 degrees with XY gap of 0.31 mm and spacing of 6.00 mm was applied for each vessel. Other settings were 275 °C extrusion temperature, auto fan speed, randomised seam, default solid infill (100%) and 36 mm s^{-1} retraction speed. Acrylonitrile Butadiene Styrene (ABS) and Polylactic Acid (PLA) filaments of 1.75 mm diameter were purchased from RS Components (United Kingdom). Before start printing, a raft-based first layer was selected to minimize 3D printing failure and to give a better grip to the build-plate while printing. The FDM 3D printer enclosure assisted in maintaining a constant temperature during printing to avoid separation of the ABS fused layers due to fast cooling.

As far as SLA 3D printing is concerned, SLA 3D printing slicer software Preform (Formlabs, United States) at 0.1 mm of printed layer thickness were chosen as printing setups. All the tests were performed by using the Grey Resin material purchased from the manufacturer (Formlabs, United States). One click print slicing feature was selected to generate the 3D printing support and automatically orient the vessel. The printed vessel was cured in isopropyl alcohol bath for 3 minutes. A post-cure was performed under UV light source for 10 minutes.

Scanning Electron Microscope: Scanning electron microscope JSM-T100 (Jeol, Japan) was used to monitor the porosity of the 3D printed samples. All samples were gold sputtered coated with

thicknesses of 9nm for FDM and 35nm for SLA. SEM images were obtained in the secondary electron mode at 15-20 kV accelerating voltage.

Leak rate measurement: the test rig in Fig. 2 was designed and built to measure leak rates. It consists of vacuum and pressure tight components (Swagelok, United Kingdom), a pressure transducer for vacuum and overpressure (WIKA Instruments, S-20, 0.25 % accuracy, United Kingdom), a cold trap and vacuum pumps (Vuotecnica Pumpset VTS 6M down to 9 kPa and Edwards nXDS6i pump down to 1 kPa). Compressed air was used for all pressure tests and its pressure adjusted through a pressure regulating valve. Data were acquired through an Arduino board. All the vessels were connected to the test rig through a 1/8 inch NPT thread fitting. To ensure a leak-tight connection between the 3D printed vessel and the testing system, a solvent-free methacrylate thread sealant (LOCTITE 561) was applied on the thread. All the tightness tests were conducted by using the pressure drop method (pressure tightness test) or pressure rise method (vacuum tightness test). The test rig without vessel has a leak rate undetectable over 24 hours and this guarantees the accuracy of the results. An Edwards Spectron 3300 (Edwards, UK) helium leak tester was used to validate further the results from the test rig in Fig. 2.

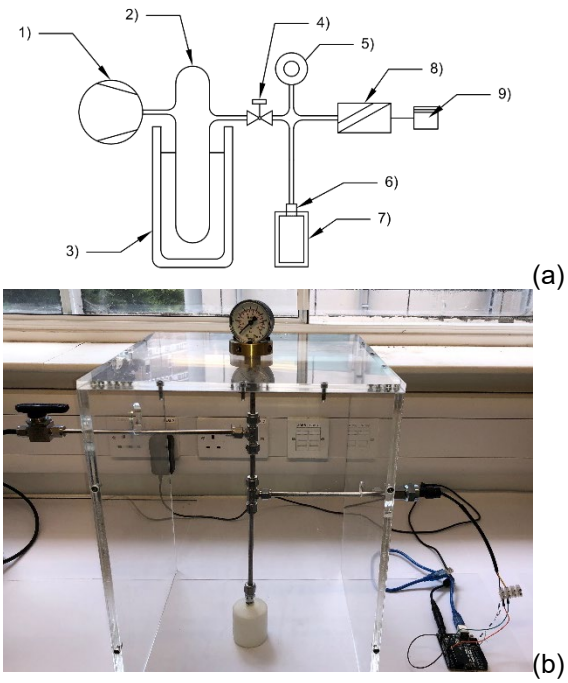

Figure 2: test rig used to measure the leak rate of 3D printed vessels. (a): the schematic diagram, (b): the build model.1) Vacuum pump or a compressor. 2) Liquid nitrogen trap. 3) Dewar flask. 4) Swagelok shut-off valve. 5) Vacuum or pressure gauge. 6)1/8 NPT fitting. 7) 3D printed vessel. 8) Pressure transmitter. 9) Data acquisition board and a computer.

Vessels: FDM sample vessel was of cylindrical shape with height of 30 mm, external diameter of 30 mm and wall thickness of 6 mm, resulting in an internal volume of 4.52 ml. SLA samples were cylindrical with one flat end and one domed end. Two samples were tested, SLA sample A was a smaller vessel with height of 40 mm, external diameter of 40 mm and wall thickness of 4 mm, resulting in an internal volume of 21.4 ml. SLA sample B was approximately one order of magnitude larger than sample A with height of 70 mm, external diameter of 60 mm and wall thickness of 4 mm, resulting in an internal volume of 113.3 ml. Further details and figures of the vessels are reported in the support material S1.

3. Tightness of FDM 3D printed vessels

Scanning electron microscopy (SEM) is used to evaluate the quality of layer bonding, and visualize the eventual porosity of FDM and SLA 3D printed samples. Fig. 3 shows the SEM images of the PLA samples and highlights the weak interlinking between layers. The fusion process leaves extra air pockets and material porosity in the structure even at 100% infill and default printing speed of 60 mm s^{-1} (recommended for PLA filaments).

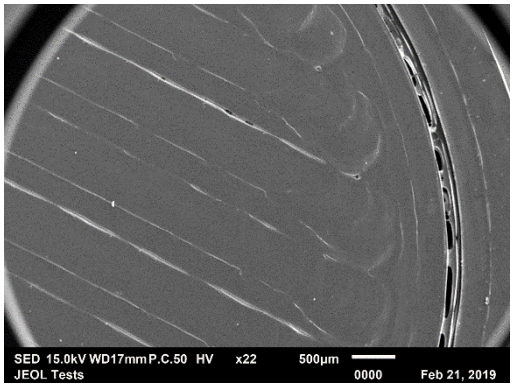

(a)
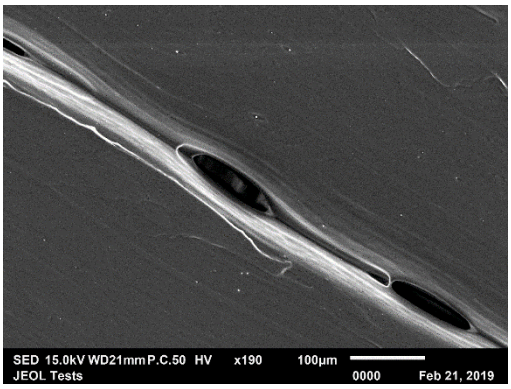

(b)

Figure 3: Scanning Electron Microscopy pictures of a 3D printed PLA sample. a) sample printed with 60 mm s^{-1} speed and 100% solid infill; b) 190X magnification on a porous area.

SEM images of FDM 3D printed ABS samples (Fig. 4) show better layer bonding than in PLA samples. Despite the excellent layer adhesion of the ABS samples, the sample shows fibres and porosity. A reduction in printing speed to 30 mm s^{-1} makes the top surface of the sample much smoother. Although ABS has good layer bonding, its porous structure, as visible under the top surface (Fig. 4d), should be completely eliminated to produce tight 3D printed vessels.

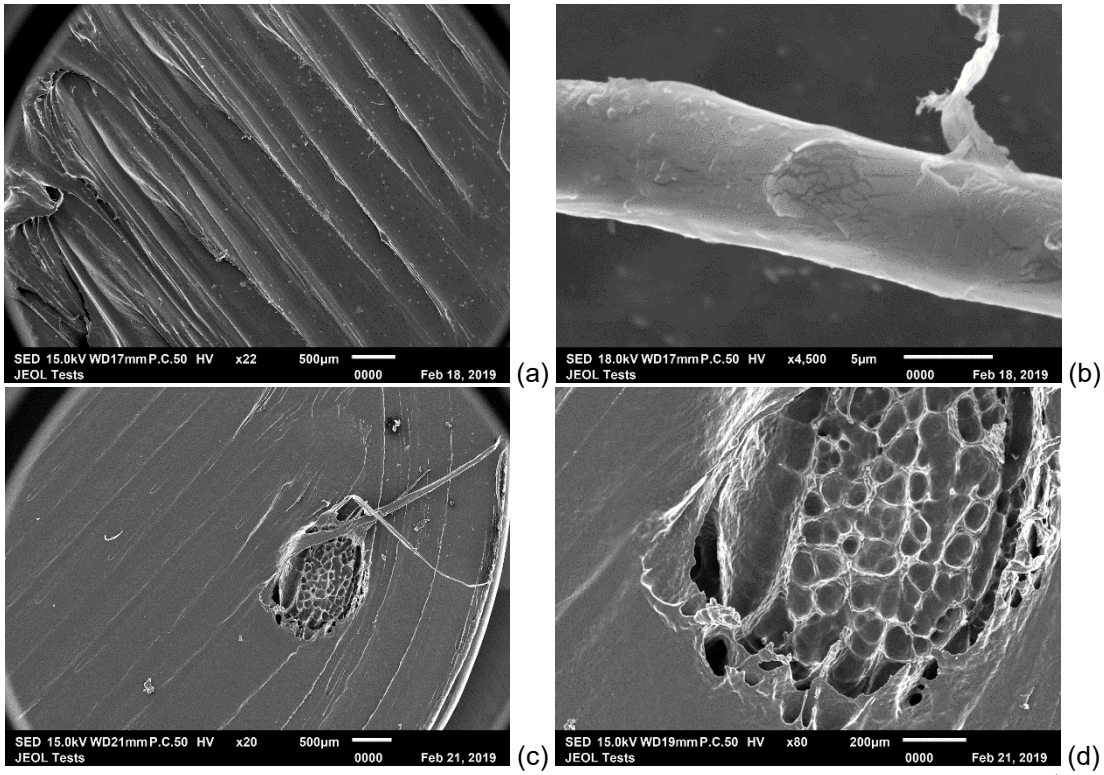

Figure 4: Scanning electron microscope images of two ABS samples. Sample 1 is printed at 60 mm s^{-1} speed while Sample 2 is printed at 30 mm s^{-1} speed. a) Sample 1 surface showing the presence of fibres; b) 4500X magnification of Sample 1 shows the presence of fibres; c) surface of Sample 2; d) 80X magnification detail of Sample 2 reveals an inner porous structure.

A reduction of the porosity of FDM 3D printed vessels is possible by tuning the printing conditions. A series of vessels of 30 mm outer diameter, 30 mm height and a 6 mm wall thickness (internal volume 4.52 ml) were printed at different conditions. The parameters selected were: i) height of each printed layer (layer height) and; ii) the amount of flowing material at each printed layer (extrusion flow). These parameters were varied in the range reported in Table 3 to assess their influence on the leak rate. The analysis focused on pressure tightness. Each vessel was pressurised with compressed air at 470 kPa. After that, the system was isolated, and the pressure change monitored over time. Results from this analysis are reported in Table 3.

Table 3: Results of the sensitivity analysis on the pressure tightness

Run	Layer height (mm)	Extrusion flow (%)	Pressure drop duration	Leak rate [Pa m^3 s^{-1}]	Tightness
1	0.09	100	435 seconds	$4.87 \cdot 10^{-3}$	Leaky
2	0.14	100	277 seconds	$7.76 \cdot 10^{-3}$	Leaky
3	0.19	100	133 seconds	$1.59 \cdot 10^{-2}$	Leaky
4	0.09	100	435 seconds	$4.87 \cdot 10^{-3}$	Leaky
5	0.09	105	1.32 hours	$3.94 \cdot 10^{-4}$	Leaky
6	0.09	110	24 hours	$1.51 \cdot 10^{-5}$	Leaky

In all the runs, the vessels resulted leaky with the worst performance when the vessel was printed at 0.19 mm layer height. This produced an extremely porous object with air voids in between the 3D printed layers. These results agree with [13], where the extrusion flow had also most dominant effect over the porosity of the 3D printed parts. Although an increase in extrusion flow can prolong the pressure drop to 24 hours, the tightness is not yet within the range of a tight system ($<10^{-6}$ Pa m^3 s^{-1}). From Table 4 the influence of layer height and extrusion flow can be quantified. As far as the layer height is concerned, the last reduction obtained in the leak rate is 5.8 10^{-2} Pa m^3 s^{-1} mm^{-1}. Therefore, even printing layers of order of microns height would not lead to any significant advantage in tightness. The extrusion flow can instead provide an average reduction of the leak rate of 4.8 10^{-4} Pa m^3 s^{-1} per percentage of increase in the extrusion flow. Unfortunately, printing at extrusion flow percentages >15% is not technically viable as evidenced by the trials reported in the support material S1.

3.1 Tightness of resin—infused FDM 3D printed vessels

Resin infusion [28] is a manufacturing technique potentially applicable for sealing FDM vessels where a resin permeates through the porous structure and fills its voids. A liquid epoxy resin (Captain Tolley) with special features of self-infusion in voids up to 1 mm diameter by capillary action was used. The resin was spread externally to the vessel and the penetration and curing processes were allowed to fully develop in 48 hours. A comparison between bubble tests of resin-infused and non-resin-infused vessels is visible in the support materials S1 and shows that resin infusion allows the vessels to be compliant with the bubble test. In Table 4 results on the test rig show that resin-infused vessels cannot be classified as vacuum or pressure tight since the leak rate remains always > 10^{-6} Pa m^3 s^{-1}, although the leak rate values are below those in Table 4 and close to acceptability.

Table 4: tightness tests of resin-infused FDM 3D printed vessels. Pressure trends are in Fig. 6.

3D printing	Initial Pressure or Vacuum	Measurement duration	Leak rate [Pa m^3 s^{-1}]	System Classification
FDM-resin infused/Pressure tightness	412 kPa	24 hours	$1.16 \cdot 10^{-5}$	Leaky
FDM-resin infused/Vacuum tightness	8.2 kPa	24 hours	$2.36 \cdot 10^{-6}$	Leaky

4. Tightness of SLA 3D printed vessels

Differently from FDM, SLA 3D printing can manufacture pore-free structures as highlighted by the SEM images of Fig. 5. Accordingly, SLA appears to be more suitable than FDM for production of tight

vessels. This pore-free structure is achieved thanks to the UV polymerisation of the epoxy-based resin.

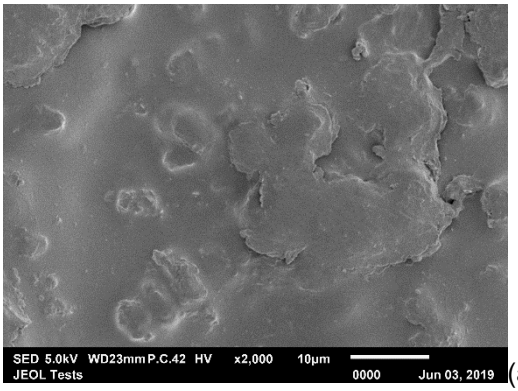

(a)
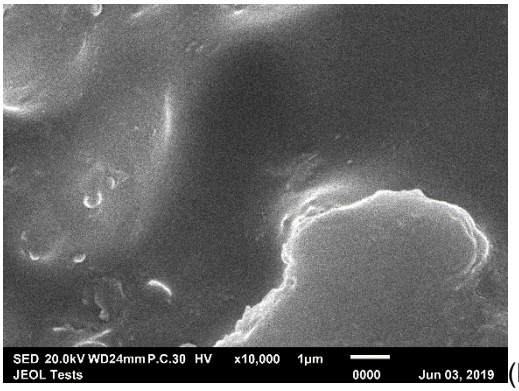

(b)

Figure 5: SEM images of one SLA 3D printed samples. a) 2000X magnification; b) 10000X magnification.

The leak rate of two SLA vessels of different size was assessed. Both samples consisted of cylindrical vessels with one flat end and one domed end. With details reported in Materials and Methods section. SLA sample A (internal volume of 21.4 ml) was tested at pressure of ~400 kPa (pressure tightness test) and vacuum of ~9 kPa and the pressure inside the vessel was monitored for 24 hours (Fig. 6). Table 5 reports the leak rate of these two tests showing that in both cases the system was very tight. Since water sorption chillers work at pressures of ~1kPa, the pressure was further reduced to this value and monitored for 250 hours. The leak rate from this last test was $2.38 \cdot 10^{-9}$ [Pa m^3 s^{-1}], fulfilling the requirements of a practical technological device. After the successful tests on the SLA sample A, a larger vessel, SLA sample B (internal volume of 113.3 ml), was tested only under vacuum for 109 hours. In this case the leak rate was at levels undetectable by the pressure rise method. Both SLA samples A and B were further helium-leak-tested in order to check the results of the pressure rise method. As Table 5 shows, the leak rates in the helium leak tests confirmed that both the vessels were very tight.

Table 5: results from the tightness tests on SLA 3D printed vessels

3D printing	Level of Pressure or Vacuum	Measurement duration	Leak rate [Pa m^3 s^{-1}]	System Classification
SLA sample A/Pressure tightness	434 kPa	24 hours	$4.95 \cdot 10^{-8}$	Very tight
SLA sample A/Vacuum tightness	8.9 kPa	24 hours	undetectable	Very tight
SLA sample A/Vacuum tightness	1 kPa	250 hours	$2.38 \cdot 10^{-9}$	Very tight
SLA sample A/Vacuum tightness	Helium leak test	--	$1.85\ 10^{-9}$	Very tight
SLA sample B/Vacuum tightness	1 kPa	109 hours	undetectable	Very tight
SLA sample B/Vacuum tightness	Helium leak test	--	$2.22\ 10^{-8}$	Very tight

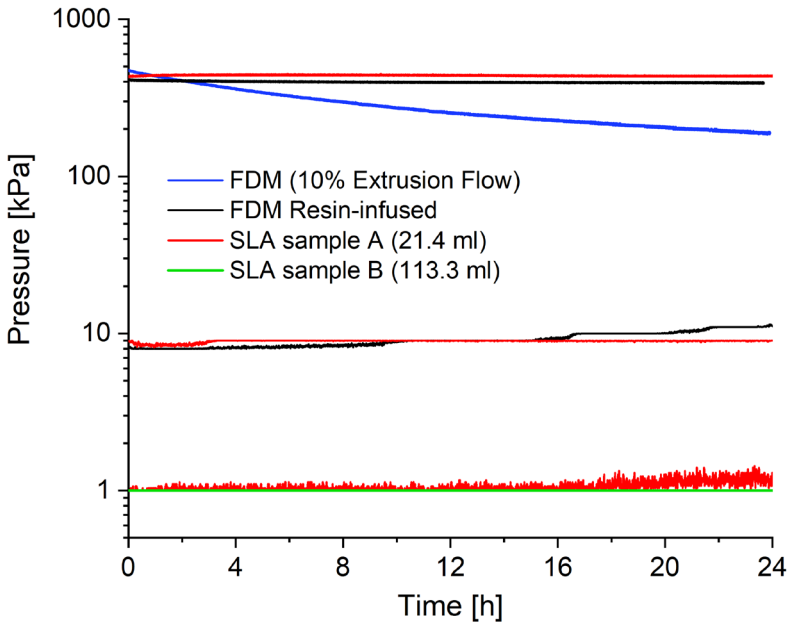

Figure 6: Pressure and vacuum tightness tests of FDM and SLA 3D printed vessels.

Conclusion

Adsorption chillers work under vacuum or pressure. Their expensive manufacturing process calls for cheap and straightforward alternatives. This investigation has focused on 3D printing manufacturing to check its suitability for adsorption chillers and heat pumps. Pressure and vacuum tightness of Acrylonitrile butadiene styrene or Polylactic Acid Fused Deposition Modelling (FDM) and Acrylates Stereolitography (SLA) 3D printed vessels were assessed. Porosity is directly correlated to tightness and was assessed through Scanning Electron Microscopy (SEM). SEM showed that SLA 3D printing produces pore-free structures. Conversely, FDM 3D printing produces structures in which the porosity can be minimized but not eliminated by optimizing the printing parameters, e.g. maximizing the extrusion flows. To mitigate this limitation, a composite resin-infused FDM 3D printed structure was realised. This process decreased the leak rate of 12 times compared to non-infused FDM vessel although this was not enough to be compatible with the specific application ultimate focus of this investigation. The results suggest that standard SLA technology can produce small-scale pressure tight vessels with leak rates in the order of 10^{-8} Pa m^3 s^{-1} and vacuum tight vessels with leak rates in the order of 10^{-9} Pa m^3 s^{-1}. These rates are compliant with the most strict tightness requirements for manufacturing adsorption chillers and heat pumps. Furthermore, provided that the mechanical requirements are met, at the pressure levels tested in this investigation the tightness does not depend

on the material rather on the porosity introduced or not by the manufacturing process. FDM lays down polymer filaments one next to the other. Unavoidably this leaves voids during printing. In SLA polymerization happens homogeneously on a plane and each plane polymerizes while a new layer is forming. In this case void-free parts can be manufactured.

References

[1] F. Meunier, Adsorption heat powered heat pumps, Appl. Therm. Eng. 61 (2013) 830–836. doi:10.1016/J.APPLTHERMALENG.2013.04.050.

[2] T. Núñez, W. Mittelbach, H.-M. Henning, Development of an adsorption chiller and heat pump for domestic heating and air-conditioning applications, Appl. Therm. Eng. 27 (2007) 2205–2212. doi:10.1016/J.APPLTHERMALENG.2005.07.024.

[3] S. Vasta, V. Palomba, A. Frazzica, G. Di Bella, A. Freni, Techno-Economic Analysis of Solar Cooling Systems for Residential Buildings in Italy, J. Sol. Energy Eng. 138 (2016) 031005. doi:10.1115/1.4032772.

[4] G. Santori, C. Di Santis, Optimal fluids for adsorptive cooling and heating, Sustain. Mater. Technol. 12 (2017). doi:10.1016/j.susmat.2017.04.005.

[5] B. Dawoud, On the development of an innovative gas-fired heating appliance based on a zeolite-water adsorption heat pump; system description and seasonal gas utilization efficiency, Appl. Therm. Eng. 72 (2014) 323–330. doi:10.1016/J.APPLTHERMALENG.2014.09.008.

[6] A. Mitchell, U. Lafont, M. Hołyńska, C. Semprimoschnig, Additive manufacturing — A review of 4D printing and future applications, Addit. Manuf. 24 (2018) 606–626. doi:10.1016/j.addma.2018.10.038.

[7] A. 1. Patwardhan, How 3D Printing Will Change the Future of Borrowing Lending and Spending?, in: Handb. Blockchain, Digit. Financ. Incl., Elsevier, 2017: pp. 493–520. doi:10.1016/B978-0-12-812282-2.00022-X.

[8] T.D. Ngo, A. Kashani, G. Imbalzano, K.T.Q. Nguyen, D. Hui, Additive manufacturing (3D printing): A review of materials, methods, applications and challenges, Compos. Part B Eng. 143 (2018) 172–196. doi:10.1016/j.compositesb.2018.02.012.

[9] J.P. Martins, M.P.A. Ferreira, N.Z. Ezazi, J.T. Hirvonen, H.A. Santos, 3D printing: Prospects and challenges: Smart 3D printing and nanomaterials for tissue regeneration, in: Nanotechnologies Prev. Regen. Med. An Emerg. Big Pict., Elsevier, 2017: pp. 299–349. doi:10.1016/B978-0-323-48063-5.00004-6.

[10] A. Pavlosky, J. Glauche, S. Chambers, M. Al-Alawi, K. Yanev, T. Loubani, Validation of an effective, low cost, Free/open access 3D-printed stethoscope, PLoS One. 13 (2018) e0193087. doi:10.1371/journal.pone.0193087.

[11] A.C. Brown, D. De Beer, Development of a stereolithography (STL) slicing and G-code generation algorithm for an entry level 3-D printer, in: IEEE AFRICON Conf., IEEE, 2013: pp. 1–5. doi:10.1109/AFRCON.2013.6757836.

[12] W. Oropallo, L.A. Piegl, Ten challenges in 3D printing, Eng. Comput. 32 (2016) 135–148. doi:10.1007/s00366-015-0407-0.

[13] E.G. Gordeev, A.S. Galushko, V.P. Ananikov, Improvement of quality of 3D printed objects by elimination of microscopic structural defects in fused deposition modeling, PLoS One. 13 (2018) e0198370. doi:10.1371/journal.pone.0198370.

[14] J.R.C. Dizon, A.H. Espera, Q. Chen, R.C. Advincula, Mechanical characterization of 3D-printed polymers, Addit. Manuf. 20 (2018) 44–67. doi:10.1016/j.addma.2017.12.002.

[15] A.E. Jakus, N.R. Geisendorfer, P.L. Lewis, R.N. Shah, 3D-printing porosity: A new approach to creating elevated porosity materials and structures, Acta Biomater. 72 (2018) 94–109. doi:10.1016/j.actbio.2018.03.039.

[16] S. Martínez-Pellitero, M.A. Castro, A.I. Fernández-Abia, S. González, E. Cuesta, Analysis of influence factors on part quality in micro-SLA technology, Procedia Manuf. 13 (2017) 856–863. doi:10.1016/j.promfg.2017.09.143.

[17] A. Farzadi, M. Solati-Hashjin, M. Asadi-Eydivand, N.A.A. Osman, Effect of layer thickness and printing orientation on mechanical properties and dimensional accuracy of 3D printed porous

samples for bone tissue engineering, PLoS One. 9 (2014) e108252. doi:10.1371/journal.pone.0108252.
[18] M. Faes, H. Valkenaers, F. Vogeler, J. Vleugels, E. Ferraris, Extrusion-based 3D printing of ceramic components, in: Procedia CIRP, Elsevier, 2015: pp. 76–81. doi:10.1016/j.procir.2015.04.028.
[19] Formlabs, The Ultimate Guide to Stereolithography (SLA) 3D Printing (Updated for 2019) | Formlabs, (2019).
[20] all3dp, Live Z axis improvement 12 Easy 3D Printing Tips on How to Improve 3D Print Quality | All3DP, (n.d.).
[21] J.T. Belter, A.M. Dollar, Strengthening of 3D printed fused deposition manufactured parts using the fill compositing technique, PLoS One. 10 (2015) e0122915. doi:10.1371/journal.pone.0122915.
[22] A. Calcatelli, M. Bergoglio, D. Mari, Leak detection, calibrations and reference flows: Practical example, Vacuum. 81 (2007) 1538–1544. doi:10.1016/j.vacuum.2007.04.019.
[23] L. Verheyden, K. Klein, C. Croué, Measurement of helium leaks 10-5 times better than the sensitivity of a mass spectrometer leak detector, Vacuum. 21 (1971) 545–549. doi:10.1016/0042-207X(71)91570-3.
[24] G. Reich, Leak detection with tracer gases; sensitivity and relevant limiting factors, Vacuum. 37 (1987) 691–698. doi:10.1016/0042-207X(87)90056-X.
[25] B. Gu, X. Huang, Investigation of leak detection method by means of measuring the pressure increment in vacuum, Vacuum. 80 (2006) 996–1002. doi:10.1016/j.vacuum.2006.01.005.
[26] K. Zapfe, Leak detection, in: CAS 2006 - Cern Accel. Sch. Vac. Accel. Proc., CERN, 2007: pp. 227–240. doi:10.5170/CERN-2007-003.227.
[27] M.P. Petkov, D.M. Soules, UHV system for quasistatic characterization of adsorbers for medium vacuum applications, Vacuum. 151 (2018) 254–260. doi:10.1016/J.VACUUM.2018.02.032.
[28] W. Obande, D. Mamalis, D. Ray, L. Yang, C.M. Ó Brádaigh, Mechanical and thermomechanical characterisation of vacuum-infused thermoplastic- and thermoset-based composites, Mater. Des. 175 (2019) 107828. doi:10.1016/j.matdes.2019.107828.